JOURNAL OF SOLID STATE CHEMISTRY **131,** 305–309 (1997)
ARTICLE NO. SC977384

The Crystal Structure of Ca_3ReO_6

A. M. Abakumov, R. V. Shpanchenko, and E. V. Antipov[1]

Department of Chemistry, Moscow State University, 119899 Moscow, Russia

and

O. I. Lebedev[2] and G. Van Tendeloo

EMAT, University of Antwerp (RUCA), Groenenborgerlaan 171, B-2020 Antwerp, Belgium

Received September 20, 1996; in revised form March 3, 1997; accepted March 11, 1997

The complex oxide Ca_3ReO_6 was synthesized and its crystal structure determined using X-ray powder analysis (space group $P2_1/n$; $a = 5.53664(5)$ Å; $b = 5.80322(5)$ Å; $c = 7.98492(7)$ Å; $\beta = 90.073(1)°$; $R_I = 0.032$, $R_P = 0.069$, $R_{wP} = 0.095$; $Z = 2$). The real symmetry is monoclinic due to a simultaneous tilt and rotation of the CaO_6 and ReO_6 octahedra. Electron diffraction and electron microscopy confirm the X-ray results. Ca_3ReO_6 is isostructural with A_2RRuO_6 oxides. © 1997 Academic Press

INTRODUCTION

At present, only a few double oxides of alkaline-earth metals and Re(VI) have been reported in the literature and only some of them have undergone a reliable structural characterization. Re(VI) cations adopt an octahedral oxygen environment and the ReO_6 octahedron is the major structural unit for these compounds. The crystal structure of $M_3Re_2O_9$ ($M = Ba, Sr$) oxides (1, 2) is based on a $9R(chh)_3$ close-packed stacking of the MO_3 layers where Re atoms occupy the octahedral interstices. Three ReO_6 octahedra are face sharing and these chains are linked by a common oxygen atom. The middle octahedron in the chain remains empty due to a strong electrostatic repulsion between high charged Re cations. The Ba_2ReO_5 compound (3), isostructural with Ba_2WO_5 (4), contains ReO_6 octahedra linked by common corners and forms infinite *cis*-bridged chains which are held together by Ba atoms.

The Ca_3ReO_6 compound was reported previously (5, 6) as a member of the perovskite-related A_2BReO_6 structural family although there is no full structural information for this compound. Moreover, there are significant discrepancies between the unit cell parameters for Ca_3ReO_6 determined by different authors. Sleight (5) indexed its powder pattern on an orthorhombic unit cell with the parameters $a = \sqrt{2}\,a_{per}$, $b = \sqrt{2}\,a_{per}$, and $c = 2\,a_{per}$ (where a_{per} is the perovskite subcell parameter) but Chamberland (6) reported a doubling of all parameters. Anderson *et al.* (7) showed that perovskites with the general formula $A_2BB'O_6$, where chess-board ordering of B cations occurs in structures with the superlattice parameters $a = \sqrt{2}\,a_{per}$, $b = \sqrt{2}\,a_{per}$, and $c = 2a_{per}$, have monoclinic symmetry due to simultaneous rotation and tilt of $B(B')O_6$ octahedra. As was found earlier from neutron diffraction data, A_2RRuO_6 ($A = Ca, Sr$; $R = La, Nd, Er, Ho, Lu, Y$) oxides have a monoclinic cell with the same set of lattice parameters and a monoclinic angle close to 90° (8–11). Therefore, taking into account the similarity of the composition and cell parameters one can expect that the Ca_3ReO_6 oxide belongs to the same family of perovskite-like compounds. The goal of the present work was to perform a detailed structural investigation of the Ca_3ReO_6 oxide using X-ray powder diffraction, electron diffraction, and high-resolution electron microscopy.

EXPERIMENTAL

CaO and ReO_3 oxides were chosen as starting materials for the synthesis of Ca_3ReO_6. CaO was obtained by decomposition of $CaCO_3$ at 1100°C for 20 h in air. The decomposition of rhenium oxomethylate $Re_4O_2(OCH_3)_{16}$, obtained by the technique described in (12), at 300°C for 3 h in air led to a pure ReO_3. Stoichiometric amounts of initial reagents were mixed, ground in an agate mortar, pressed into 0.4 g pellets, and placed in alumina crucibles to avoid reaction with the silica tube. The samples were sealed in evacuated silica tubes with 5–7 cm^3 volume at 10^{-2} Torr

---

[1] To whom correspondence should be addressed.

[2] On leave from Institute of Crystallography, Russian Academy of Science, 117333 Moscow, Russia.

0022-4596/97 $25.00

pressure. The annealing was carried out at 800°C for 40 h. After all samples were annealed, they were furnace cooled.

Phase compositions and lattice parameters were determined using X-ray powder diffraction data (Cu$K\alpha_1$ radiation, $\lambda = 1.54056$ Å) obtained with a focusing Guinier-camera FR-552 (Ge was used as an internal standard). Raw data for crystal structure determination were collected using a STADI/P diffractometer (CU$K\alpha_1$ radiation, curved Ge monochromator, transmission mode, step 0.02° (2θ), scintillation counter).

The powder crystal structure refinements were carried out using the RIETAN-97 program. The Rietveld method with a modified pseudo-Voight profile function was used for the final refinement.

The electron diffraction and EDX analysis were done on a Philips CM20 microscope, operating at 200 kV and equipped with a LINK-2000. High-resolution electron microscopy was performed on a JEOL 4000EX electron microscope, operating at 400 kV. Image simulations were carried out using the MacTempas software.

RESULTS AND DISCUSSION

1. X-ray Diffraction Study

The Ca_3ReO_6 compound was prepared with insignificant amounts of an undefined impurity (maximal intensity of the admixture peak was less than 5% of the intensity of the strongest peak). The X-ray powder diffraction pattern was indexed on an orthorhombic unit cell with the parameters $a = 5.5359(1)$ Å, $b = 5.8024(1)$ Å, and $c = 7.9836(2)$ Å. This type of distortion of the perovskite subcell is consistent with the value of the Goldshmidt factor $t = 0.9$ calculated from the ionic radii given by Shannon *et al.* (13). The only $h0l$: $h + l = 2n$ systematic extinction was unambiguously detected. It allowed us to propose as possible space groups *Pmmn* or $Pmn2_1$. The presence of $0kl$: $k = 2n + l$ reflections provides the evidence that this structure does not belong to the $GdFeO_3$ type (14) and the placement of *B* cations is ordered and not random. The initial model for the refinement was based on the perovskite structure where *B* positions are occupied by Ca and Re in a chess-board order and the remaining Ca atoms are located in *A* positions. However, the subsequent refinement of this model led to high values of reliability factors ($R_I > 0.08$), unreasonable thermal parameters for the oxygen atoms, and metal–oxygen distances. It indicates that the real crystal symmetry may be lower than orthorhombic or an increase in unit cell dimensions is needed. Nevertheless, the structural refinement confirmed a chess-board ordered placement of *B* cations and indicated that an anion sublattice distortion could not be determined perfectly within the orthorhombic unit cell described above.

As shown by Anderson *et al.* (7), there are no examples where chess-board ordering of *B* cations occurs in structures belonging to an orthorhombic crystal system with the superlattice parameters $a = \sqrt{2}\,a_{\mathrm{per}}$, $b = \sqrt{2}\,a_{\mathrm{per}}$, and $c = 2a_{\mathrm{per}}$. This type of perovskite structure distortion arises when the *A*–O distance divided by $\sqrt{2}$ is less than the *B*–O bond length, i.e., when the Goldshmidt tolerance factor is less than 1. The decrease in coordination number of small *A* cations requires the distortion of the initial perovskite oxygen framework which may be realized by the rotation of the BO_6 octahedra around $[100]_{\mathrm{per}}$ together with a tilt around $[011]_{\mathrm{per}}$. However, the possible topological transformations of the perovskite structure do not allow a chess-board ordering of the *B* cations simultaneously with a rotation and tilting of the BO_6 octahedra in the $a = \sqrt{2}\,a_{\mathrm{per}}$, $b = \sqrt{2}\,a_{\mathrm{per}}$, and $c = 2a_{\mathrm{per}}$ orthorhombic unit cell (15). A detailed structural investigation of such compounds should reveal an expansion of the unit cell or the existence of a monoclinic distortion where the monoclinic angle is close to 90°. We failed to detect reflections on the X-ray pattern which could arise from an increase in cell parameters. The further refinements were therefore made using a monoclinic unit cell, despite the fact that the X-ray diffraction pattern was successfully indexed in terms of the orthorhombic unit cell. According to the observed extinction condition, the $P2_1/n$ and $P2/n$ space groups are possible. The space group symmetry $P2_1/n$ and initial atomic coordinates were

TABLE 1
Crystallographic Parameters for Ca_3ReO_6

Space goup	$P2_1/n$
a, Å	5.53664(5)
b, Å	5.80322(5)
c, Å	7.98492(7)
β, deg.	90.073(1)
Cell volume, Å^3	256.588(7)
Z	2
2θ-range, time/step	15°–120°, 50 s
Number of reflections	379
Refinable parameters	39
Reliability factors	$R_I = 0.032$, $R_P = 0.069$, $R_{wP} = 0.095$

TABLE 2
Positional and Thermal Parameters for Ca_3ReO_6

Atom	Position	x/a	y/b	z/c	B_{iso}, Å^2
Ca(1)	4*e*	0.5179(8)	0.5590(3)	0.7459(3)	1.52(2)
Ca(2)	2*c*	1/2	0	1/2	1.32(5)
Re	2*d*	1/2	0	0	0.90(1)
O(1)	4*e*	0.217(1)	0.177(1)	0.048(1)	0.6(2)
O(2)	4*e*	0.337(1)	0.721(1)	0.066(1)	0.6(2)
O(3)	4*e*	0.395(1)	0.947(1)	0.7710(9)	0.9(2)

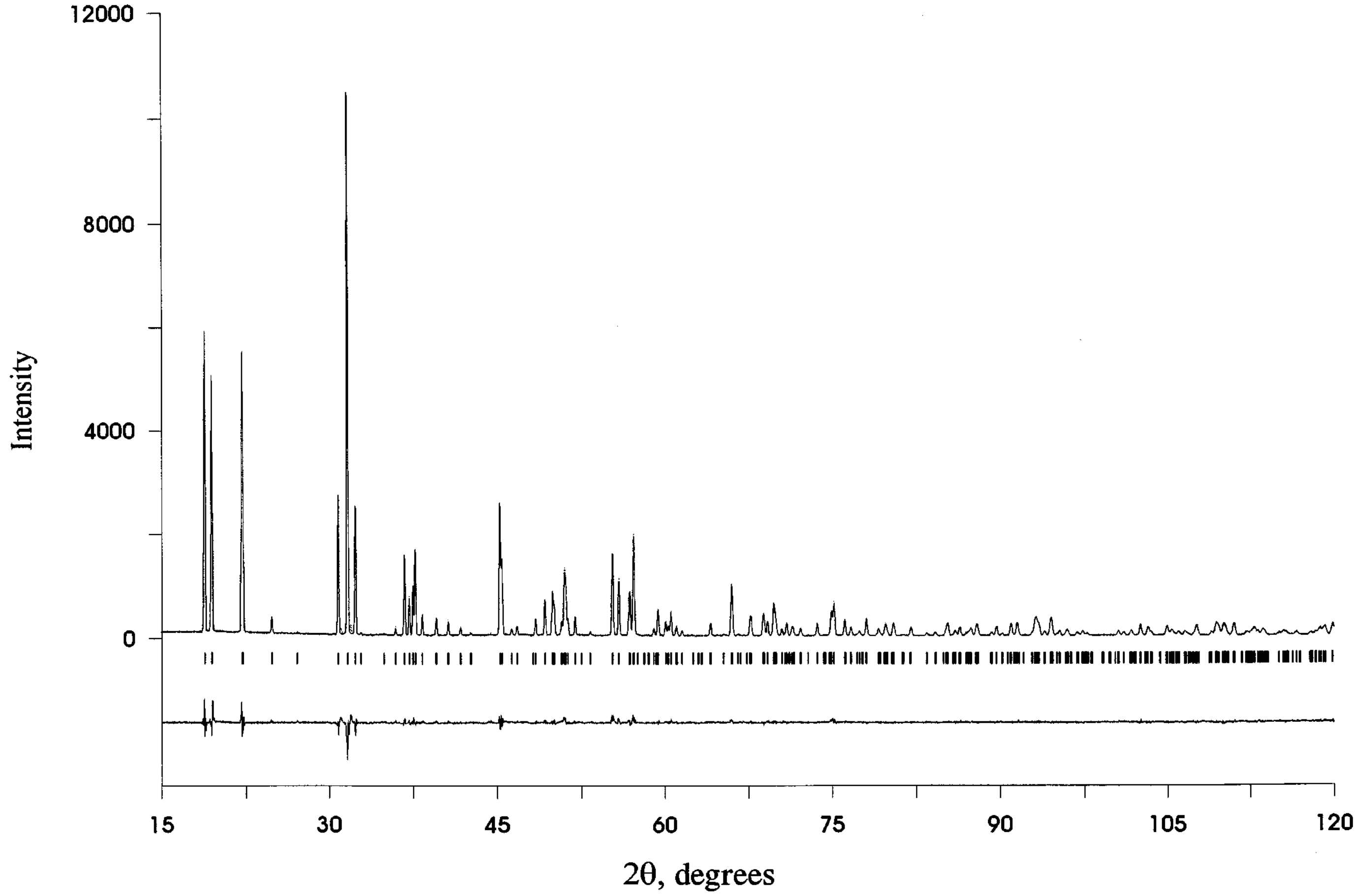

FIG. 1. Observed and difference X-ray patterns for Ca_3ReO_6.

taken from the Ca_2LaRuO_6 crystal structure (8). The final refinement was carried out in an isotropic approximation of the thermal parameters. Thermal parameters for oxygen atoms were refined independently. Before the refinement, the impurity peaks were removed from the raw data by profile analysis since they did not overlap with peaks from the main phase. After several refinement cycles reasonable values of reliability factors were obtained: $R_I = 0.032$, $R_P = 0.069$, $R_{wP} = 0.095$. The observed and difference X-ray patterns are shown in Fig. 1. The crystallographic parameters, positional parameter, and selected interatomic distances for Ca_3ReO_6 are listed in Tables 1, 2, and 3, respectively.

TABLE 3
Main Interatomic Distances (Å) and Angles (deg.) for Ca_3ReO_6

Ca(1)–O(1)	2.365(7) × 1	Ca(1)–O(3)	2.361(6) × 1	Re–O(2)	1.927(6) × 2
Ca(1)–O(1)	2.684(7) × 1	Ca(1)–O(3)	2.380(7) × 1	Re–O(3)	1.943(7) × 2
Ca(1)–O(1)	2.768(8) × 1	Ca(2)–O(1)	2.259(6) × 2		
Ca(1)–O(2)	2.353(7) × 1	Ca(2)–O(2)	2.324(6) × 2		
Ca(1)–O(2)	2.612(7) × 1	Ca(2)–O(3)	2.262(7) × 2		
Ca(1)–O(2)	2.903(8) × 1	Re–O(1)	1.913(6) × 2		
O(1)–Ca(2)–O(1)	180.0(2)	O(1)–Re–O(1)	180.0(3)		
O(2)–Ca(2)–O(2)	180.0(2)	O(2)–Re–O(2)	180.0(3)		
O(3)–Ca(2)–O(3)	180.0(2)	O(3)–Re–O(3)	180.0(3)		
O(1)–Ca(2)–O(2)	90.4(2)	O(1)–Re–O(2)	89.3(3)		
O(1)–Ca(2)–O(3)	95.0(2)	O(1)–Re–O(3)	91.7(3)		
O(2)–Ca(2)–O(3)	94.9(2)	O(2)–Re–O(3)	90.9(3)		
Ca(2)–O(1)–Re	147.9(4)	Ca(2)–O(3)–Re	143.3(3)		
Ca(2)–O(2)–Re	141.0(3)				

The Ca_3ReO_6 crystal structure is shown in Fig. 2. As mentioned above, Ca and Re both occupy the octahedral interstices in an ordered manner forming a "rock salt" type cation sublattice. Re cations have an almost regular octahedral oxygen environment whereas 1/3 of the Ca atoms are located in slightly distorted octahedra. The metal–oxygen distances $d_{Ca(2)-O} = 2.26$–2.32 Å and $d_{Re\text{-}O} = 1.91$–1.94 Å correspond to the ionic radii of Ca^{2+} (1.00 Å) and Re^{6+} (0.52 Å) for $CN = 6$. Since Ca atoms are too small to be placed into 12-fold coordinated A positions, ReO_6 and CaO_6 octahedra are cooperatively tilted along $[011]_{per}$ and rotated along $[100]_{per}$ to reduce eight of the originally 12

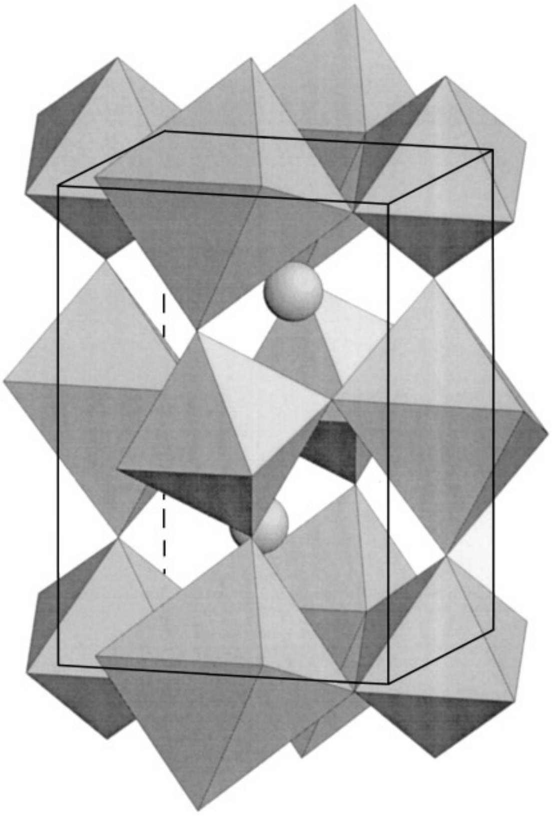

FIG. 2. Crystal structure of Ca_3ReO_6.

equal Ca(1)–O distances. The values of the bond angles Ca(2)–O–Re vary in the range 141.0°–147.9° and clearly indicate a distortion of the octahedral framework.

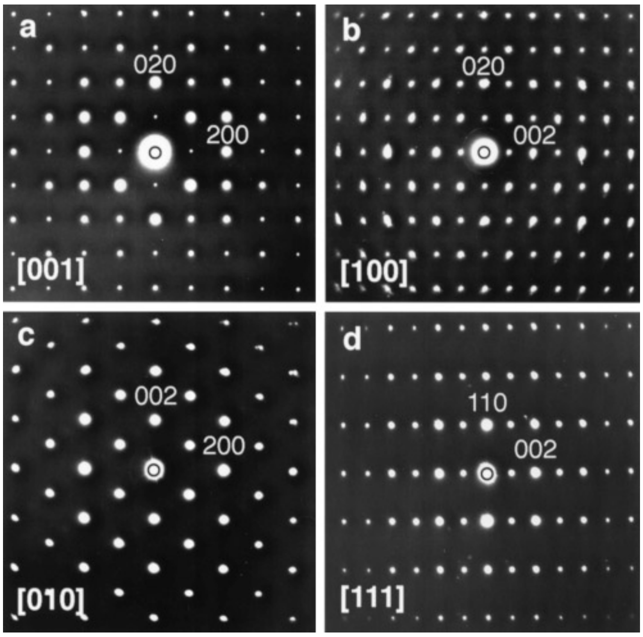

FIG. 3. Electron diffraction patterns of different reciprocal zones of Ca_3ReO_6; the zone axes and some important reflections are indicated.

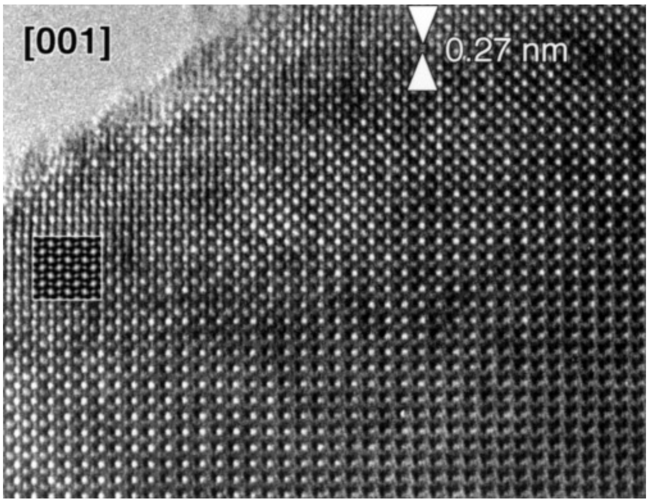

FIG. 4. HREM image of Ca_3ReO_6 along the [001] zone. The simulated image for a focus value of 70 nm and a thickness of 5 nm is shown as an inset.

2. Electron Microscopy Study

To confirm the structure determination an electron microscopy study was performed. Electron diffraction (ED) patterns of the main reciprocal zones are shown in Fig. 3. ED patterns of [001], [100], and [111] reciprocal zones do exhibit reflections with indices $h0l$: $h + l \neq 2n$, but these reflections are less intense compared to the reflections $h0l$: $h + l = 2n$ and disappear when the crystallite is tilted. They are therefore to be attributed to double diffraction. This conclusion is confirmed by the absence of any forbidden reflections in the [010] zone where double diffraction conditions do not exist.

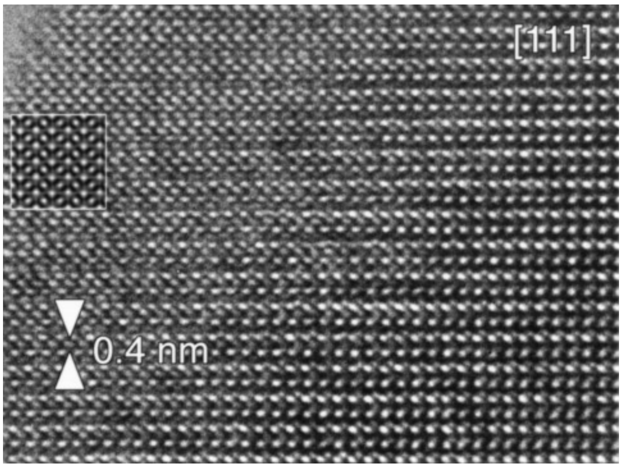

FIG. 5. HREM image of Ca_3ReO_6 along the [111] zone. The simulated image for a focus value of 70 nm and a thickness of 5 nm is shown as an inset.

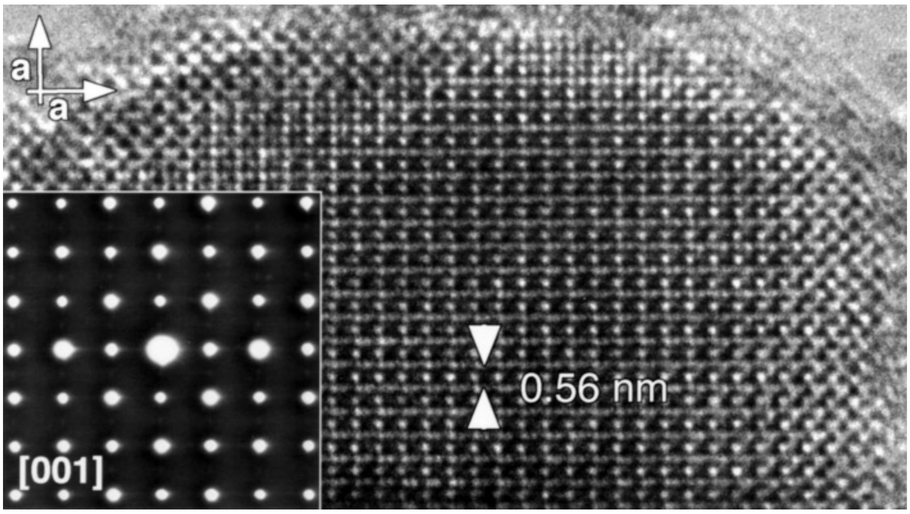

FIG. 6. HREM image and corresponding ED pattern of the $Ca_4Re_3O_x$ phase along the [001] zone.

High resolution (HREM) images of [001] and [111] zones are present in Figs. 4 and 5, respectively, and reveal a well-ordered structure. No planar defects, except twinning along the [111] axis, were observed. The twinning occurs on (112) plains because of the close d spacings of the (110) and (002) planes. Calculated images of [001] and [111] zones for different defocus values and thicknesses are in good agreement with the experimental HREM images; they are shown as an inset in Figs. 4 and 5.

The unknown impurity phase, found in the X-ray pattern, has been identified by electron microscopy. The [001]* ED pattern and the corresponding HREM image are presented in Fig. 6. The electron diffraction shows reflections closely related to those in the [001]* zone of Ca_3ReO_6 with $a = b \approx 5.6$ Å. The chemical analysis by EDX however indicated a Ca-rich compound with approximate composition $Ca_4Re_3O_x$. A more detailed study of this compound is in progress.

ACKNOWLEDGMENTS

This work was supported by the Russian Science Foundation (Grant 95-03-09484a) and an individual fellowship from the International Soros Science Education Program (a96-113). OIL is indebted to the Belgian Government, Prime Minister's Office of Science Policy Programming for this fellowship at EMAT-RUCA.

REFERENCES

1. B. L. Chamberland and F. C. Hubbard, *J. Solid State Chem.* **26,** 79 (1978).
2. C. Calvo, H. N. Ng, and B. L. Chamberland, *Inorg. Chem.* **17,** 699 (1978).
3. A. K. Cheetham and D. M. Thomas, *J. Solid State Chem.* **71,** 61 (1987).
4. L. M. Kovba, L. N. Lykova, V. L. Balashov, and A. L. Kharlanov, *Koord. Khim.* **11,** 1426 (1985).
5. A. W. Sleight, J. M. Longo, and R. Ward, *Inorg. Chem.* **1,** 245 (1962).
6. B. L. Chamberland and G. Levasseur, *Mater. Res. Bull.* **14,** 401 (1979).
7. M. T. Anderson, K. B. Greenwood, A. T. Gregg, and K. R. Poppelmeier, *Prog. Solid State Chem.* **22,** 197 (1993).
8. P. D. Battle, J. B. Goodenough, and R. J. Price, *J. Solid State Chem.* **46,** 234 (1983).
9. P. D. Battle and W. J. Macklin, *J. Solid State Chem.* **52,** 138 (1984).
10. P. D. Battle and C. W. Jones, *J. Solid State Chem.* **78,** 108 (1989).
11. P. D. Battle, C. W. Jones, and F. Studer, *J. Solid State Chem.* **90,** 302 (1991).
12. V. G. Kessler, A. V. Shevelkov, G. V. Chvoryh, G. A. Seinenbaeva, N. Ja. Turova, and D. V. Drobot, *Russ. J. Inorg. Chem.* **40,** 1477 (1995).
13. R. D. Shannon, *Acta Crystallogr. A* **36,** 751 (1976).
14. M. Marezio, J. P. Remeika, and P. D. Dernier, *Acta Crystallogr.* **26,** 2008 (1970).
15. A. M. Glazer, *Acta Crystallogr., Sect B* **28,** 3384 (1972).